

# UC Berkeley

## UC Berkeley Previously Published Works

### Title

Spatial patterning of the neonatal EEG suggests a need for a high number of electrodes

### Permalink

<https://escholarship.org/uc/item/58q0r1w9>

### Journal

NeuroImage, 68(3)

### ISSN

10538119

### Authors

Odabae, Maryam  
Freeman, Walter J, III  
Colditz, Paul B  
[et al.](#)

### Publication Date

2012-12-13

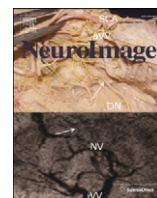
### DOI

10.1016/j.neuroimage.2012.11.062

### Copyright Information

This work is made available under the terms of a Creative Commons Attribution License, available at <https://creativecommons.org/licenses/by/3.0/>

Peer reviewed



## Spatial patterning of the neonatal EEG suggests a need for a high number of electrodes

Maryam Odabae<sup>a</sup>, Walter J. Freeman<sup>b</sup>, Paul B. Colditz<sup>a</sup>, Ceon Ramon<sup>c,d</sup>, Sampsa Vanhatalo<sup>a,e,f,\*</sup>, 1

<sup>a</sup> The University of Queensland Perinatal Research Centre and UQ Centre for Clinical Research (UQCCR), Royal Brisbane and Women's Hospital, Brisbane, Australia

<sup>b</sup> Department of Molecular and Cell Biology, University of California at Berkeley, CA 94720, USA

<sup>c</sup> Department of Electrical Engineering, University of Washington, Seattle, WA 98195, USA

<sup>d</sup> Department of Bioengineering, Reykjavik University, Reykjavik University, Iceland

<sup>e</sup> Department of Children's Clinical Neurophysiology, Helsinki University Central Hospital, Helsinki, Finland

<sup>f</sup> Department of Neurological Sciences, University of Helsinki, Finland

### ARTICLE INFO

#### Article history:

Accepted 30 November 2012

Available online 13 December 2012

#### Keywords:

High resolution EEG

SAT

Source localization

Head model

Spatial spectrum

Spatial sampling

### ABSTRACT

There is an increasing demand for source analysis of neonatal EEG, but currently there is inadequate knowledge about i) the spatial patterning of neonatal scalp EEG and hence ii) the number of electrodes needed to capture neonatal EEG in full spatial detail. This study addresses these issues by using a very high density (2.5 mm interelectrode spacing) linear electrode array to assess the spatial power spectrum, by using a high density (64 electrodes) EEG cap to assess the spatial extent of the common oscillatory bouts in the neonatal EEG and by using a neonatal size spherical head model to assess the effects of source depth and skull conductivities on the spatial frequency spectrum.

The linear array recordings show that the spatial power spectrum decays rapidly until about 0.5–0.8 cycles per centimeter. The dense array EEG recordings show that the amplitude of oscillatory events decays within 4–6 cm to the level of global background activity, and that the higher frequencies (12–20 Hz) show the most rapid spatial decline in amplitude. Simulation with spherical head model showed that realistic variation in skull conductivity and source depths can both introduce orders of magnitude difference in the spatial frequency of the scalp EEG.

Calculation of spatial Nyquist frequencies from the spatial power spectra suggests that an interelectrode distance of about 6–10 mm would suffice to capture the full spatial texture of the raw EEG signal at the neonatal scalp without spatial aliasing or under-sampling. The spatial decay of oscillatory events suggests that a full representation of their spatial characteristics requires an interelectrode distance of 10–20 mm.

The findings show that the conventional way of recording neonatal EEG with about 10 electrodes ignores most spatial EEG content, that increasing the electrode density is necessary to improve neonatal EEG source localization and information extraction, and that prospective source models will need to carefully consider the neonatally relevant ranges of tissue conductivities and source depths when source localizing cortical activity in neonates.

© 2012 Elsevier Inc. All rights reserved.

### Introduction

Recent work in neuroimaging (Dudink et al., 2012; Fransson et al., 2011; Lodygensky et al., 2010) and in developmental neurobiology

(Colonnese and Khazipov, 2012; Hanganu-Opatz, 2010; Vanhatalo and Kaila, 2010) has made it clear that brain functions are already highly specialized early in development. Functional assessment of neonatal brain activity is currently severely hampered by the poor spatial resolution provided by conventional neonatal EEG recording (Andre et al., 2010), which hardly suffices to distinguish brain lobes from each other. In order to meet the need for better spatial parcellation, several methods have been recently devised to enable recording of high density EEG (hdEEG) from the neonatal head in the laboratory environment (Fifer et al., 2006; Roche-Labarbe et al., 2008; Vanhatalo et al., 2008), and even in the neonatal intensive care unit (Stjerna et al., 2012; Vanhatalo et al., 2008).

The theoretical benefits of increasing the number of recording electrodes are clear (see e.g. Grieve et al., 2003, 2004). Improved spatial

*Abbreviations:* EDF, European Data Format; hdEEG, high density EEG; PSDx, spatial power spectral density; PSDt, temporal power spectral density; SAT, spontaneous activity transient.

\* Corresponding author at: Department of Clinical Neurophysiology, Children's Hospital, Helsinki University Hospital, PO Box 280, FIN-00029 HUS, Finland.

E-mail address: [sampsa.vanhatalo@helsinki.fi](mailto:sampsa.vanhatalo@helsinki.fi) (S. Vanhatalo).

<sup>1</sup> Current address: Perinatal Research Centre, University of Queensland Center for Clinical Research (UQCCR), Royal Brisbane and Women's Hospital (RBWH), Herston 4029, Australia.

resolution obtained from a higher number of electrodes has made it possible to record cerebral activities that were previously not known, or were difficult to localize (e.g. Scherg et al., 2002; Tucker et al., 2007). Most importantly, an increase in spatial sampling has opened the pathway to a genuine source localization of neonatal EEG (Beauchemin et al., 2011; Despotovic et al., 2012; Roche-Labarbe et al., 2008), akin to what is routinely done with adult EEG already.

It is intriguing in this context, that we do not know how much EEG information can be obtained from the baby scalp. This richness in amplitude texture can be perceived as “spatial patterning” of the neonatal scalp EEG (hereafter referred to as “spatial patterning”), and it has been measured in adults by estimating the spatial frequency content of the scalp EEG (Freeman et al., 2003; Srinivasan et al., 1998). This would be a necessary piece of information to define the number of EEG electrodes that are needed to record the brain activity in full detail, to estimate the errors related to the conventional under-sampling of EEG (see also Grieve et al., 2004), as well as to aid in constructing realistic forward and inverse solutions for neonatal EEG source localization. The spatial resolution of scalp EEG signals is impaired by smearing due to the scalp and skull. Because these barriers are of lower impedance in infants, the degradation is much less severe (see also Despotovic et al., 2012), so information about brain function is more accessible, and detailed spatial information should be readily measurable from the scalp (Grieve et al., 2003, 2004).

In this study, we explored the spatial patterning of neonatal EEG by using recordings with an ultrahigh density linear array (2.5 mm interelectrode distance) and high density (64 channel) EEG caps in healthy newborn babies. Our aim was to address two fundamental, complementary questions: i) How complex is the EEG amplitude on the neonatal scalp? and ii) How large are the oscillatory bouts measured on the neonatal scalp?

## Methods and materials

The study consists of three complementary parts. The first part uses a custom-fabricated linear array of electrodes (see also Freeman and Quiñero, *in press*; Freeman et al., 2003) to obtain a theoretical estimate of the spatial EEG patterning in selected scalp locations. The second part uses a commercial high density (hdEEG, 64 channels) EEG cap in order to estimate the spatial extent of focal fluctuations of amplitudes, and to estimate the “practical” spatial EEG extent (“patterning”) from oscillatory events in the neonatal EEG (Andre et al., 2010; Vanhatalo and Kaila, 2006 and 2010; Khazipov and Luhmann, 2006). These events appear as short bursts of higher frequency activity, often nested (Vanhatalo et al., 2005) within slow waveforms and have multiple names related to their visual appearance (e.g. delta brush, however see Table 1 in Vanhatalo and Kaila, 2010 for further considerations). In the third part, we employed a spherical head model with neonatal dimensions to see i) whether our empirically measured spatial power spectral density (PSD<sub>x</sub>) can be reproduced by using a simple parametric model, and ii) how skull layer conductivity or source depth affect the PSD<sub>x</sub>. These aimed to pilot the pathway to translate our results into future realistic head models.

### Subjects and recordings

#### Subjects

EEG recordings were obtained from term newborns ( $n = 2$  for the linear array study;  $n = 5$  for the hdEEG recordings). EEG data were recorded in the Department of Children’s Clinical Neurophysiology (Helsinki University Central Hospital) using a Cognitrace amplifier with sampling rate of 256 Hz or 512 Hz and an inbuilt average reference (ANT B.V., Enschede, The Netherlands, [www.ant-neuro.com](http://www.ant-neuro.com)). Informed consent was obtained from the parents. This study was approved by the Ethics Committee of the Hospital for Children and Adolescents, Helsinki University Central Hospital.

### Linear array recording

A linear electrode array was custom made by embedding 50 electrode pins (material Ag/AgCl; diameter 1 mm; obtained from Biomed Product, USA) into a silicone strip with a 2.5 mm interelectrode distance (Fig. 1). The linear array was interfaced with the amplifier using a flat cable attached to a standard DB37 connector. Additional ground and reference electrodes were added as conventional cup electrodes (material Au), placed on the opposite side of the head. The scalp was cleaned and dried, and the array was lightly bound over either the parietal or occipitoparietal scalp or over the fontanel (extending from about POZ position along the midline to fontanel).

### hdEEG recording

Sixty-four channel hdEEG caps were used (Waveguard, ANT B.V., Enschede, The Netherlands, [www.ant-neuro.com](http://www.ant-neuro.com); see also Stjerna et al., 2012). A video clip showing an EEG recording of this kind is shown in the link [www.nemo-europe.com/en/educational-tools.php](http://www.nemo-europe.com/en/educational-tools.php).

### Data analysis

#### Linear array experiment

Lack of gel (as in conventional EEG recordings) and the poor mechanical stability of the electrode–skin interface created a challenge for obtaining signal segments that were clean enough from artefacts. We selected epochs where there were more than twenty adjacent electrodes with sufficiently clean signal. Altogether 54 s of such EEG from seven different time windows were identified ((range 1.1–19 s; mean length 7.7 s. An  $n$  epoch is shown in Fig. 1. Epochs were exported in EDF format for further analysis after bandpass filtering at 3–30 Hz to remove mains-related artefacts and trace instability due to mechanical movements.

Single missing traces (for an example, see Fig. 1C; traces #19 and #48) were interpolated using nearest two neighbouring channels, which introduces a spatial lowpass filter, and hence a small but unavoidable underestimation of the higher spatial frequencies. Then, PSD<sub>x</sub> was calculated from the vectors created from the signal values across the channels at each sampling (see Fig. 1D; see also Freeman et al. (2003). Due to the EEG sampling frequency, this results in 256 PSD<sub>x</sub> traces per second. We then calculated the median value of each spatial frequency bin from each EEG epoch.

The use of spatial frequency spectrum to estimate the optimal electrode density (i.e. spatial frequency) can be considered analogous to the common use of temporal frequency spectrum (PSD<sub>t</sub>) to estimate the required (temporal) sampling frequency of the EEG signal. The canonical form of the spatial spectrum is three segments: a flat low-frequency segment, a middle segment with rapid fall in power with increasing frequency, and a flat high-frequency segment resembling that of white noise (see Freeman et al., 2000). Most of the desired information is contained in the middle segment between two inflections. The first step is to define the point in the spectrum where it reaches the noise floor (termed the “upper inflection point” in Results) and gives the upper end of the frequency range that should ideally be captured. The second step is to calculate the number of electrodes with the specified interelectrode spacing that are needed to sample the entire range of spatial frequency (Freeman et al., 2003; Srinivasan et al., 1998). The lower inflection point gives an estimate of the desired width of the array. According to the Nyquist theorem, more than two samples are required to capture each cycle at the highest frequency and preferably three samples are required for the “practical” Nyquist frequency). The width of the array must be great enough to encompass at least one cycle of the lowest spatial frequency. In the temporal domain, these would be cycles per second (or Hz) and recording duration in seconds, whilst in the spatial domain they are cycles per centimeter and dimensions of an array in cm. For instance, in the case of 1 cycle/cm, one should have at least two electrodes in each centimeter (i.e. 5 mm interelectrode spacing) to sample adequately the given spatial pattern in EEG oscillation. The product of the sampling frequency in number

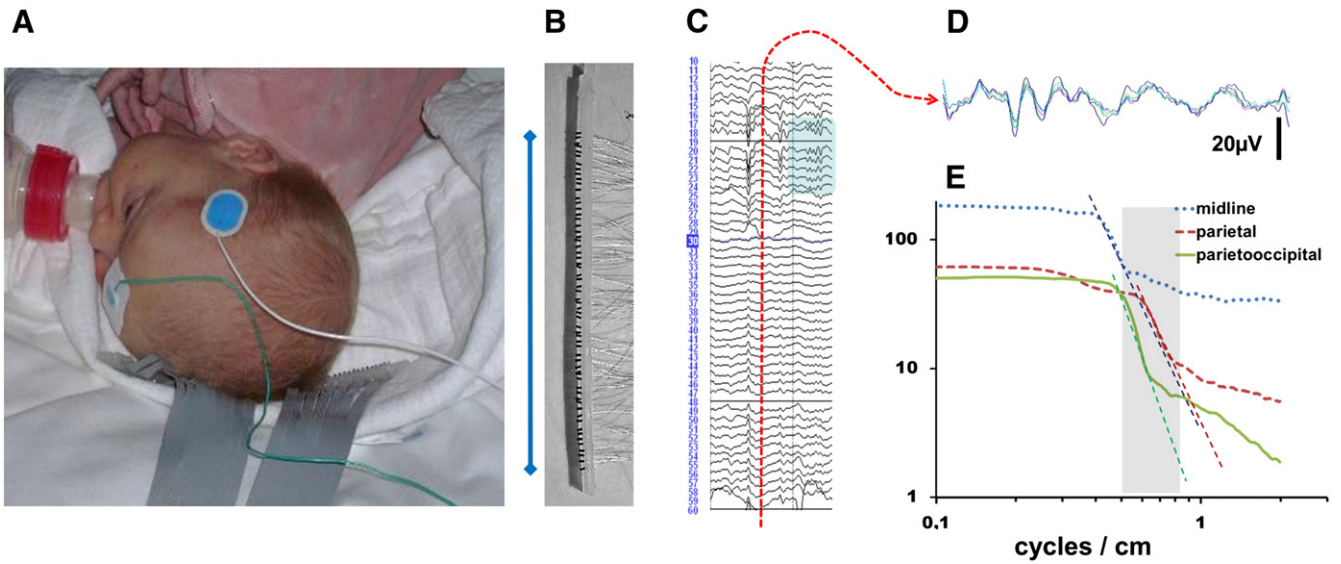


**Fig. 1.** Linear array experiment. A) Linear array device, and the ground (green wire) and reference (blue) electrodes. The white cloth was used to wrap the array tightly against the baby's scalp, shown in the parieto-occipital position in this figure. B) The structure of the linear array device in more detail. Sensor pins (1 mm thick) were placed at 2.5 mm intervals on a silicone bar. The blue vertical scale bar between photographs is 15 cm. C) Example of a segment of raw data obtained from the linear array device. Note how single transient or short oscillation (depicted with the shaded gray area) is limited to a part of the electrode array only. The stippled line shows the direction of sampling for the spatial frequency analysis. D) Examples of time series used for the analysis of spatial frequency. This time series consists of about 50 samples that were collected from a single time point over the linear array. E) Spatial spectra of linear array recordings from three different scalp locations. There is a clear roll-off of power at around 0.5–0.8 cycles/cm that is shown highlighted by the shaded area. Note the remarkably similar 1/f linear slope in the middle part between the PSDx traces from different brain areas. The PSDx traces are cut at 2 c/cm, which is the spatial Nyquist frequency in these recordings with sampling of 4 electrodes/cm.

of electrodes/cm times the width of the array in cm gives the number of electrodes and channels required.

#### Methodological considerations

It would have been obviously ideal to record with a headgear that has sensors positioned in 2D with the density used in our current linear array. Our pilot experiments with a prototype of such ultrahigh density 2D array showed that, with the technology available to us now, it was not possible to manufacture a 2D array that would be gentle enough for the neonatal scalp, and yet obtain sufficiently stable recordings. Frontal location was not used because the babies felt too uncomfortable after placing the array onto forehead, which led to excessive frontal muscle activation that would have mixed with the EEG and cannot be removed afterwards (cf. Freeman et al., 2003).

#### hdEEG experiment

We visually identified focal oscillations from epochs within EEG background classified as trace alternant, the dominant pattern during quiet sleep in neonates (Andre et al., 2010; Vanhatalo et al., 2005). This state was selected to provide better signal to noise for the subsequent analysis that targeted the bouts of rapid oscillations typically associated with SAT events (see also Tokariev et al., 2012; Vanhatalo et al., 2005). The oscillation bouts were identified after applying bandpass filtering (for reading only) into three frequency bands: 1–5 Hz, 5–10 Hz and 12–18 Hz. The filtering during visual reading was based on Butterworth forward filter with slope of 24 dB per octave built into ASA software. These frequency bands were selected to roughly correspond to the individual oscillatory components in the neonatal EEG (cf. Tokariev et al., 2012). All data were exported to EDF format and filtered at 1 Hz–20 Hz by using Butterworth forward and backward filter (zero phase) with slope of 6 dB per octave built into ASA software.

In the further, quantitative analysis, all signals were filtered into three frequency bands with FIR linear phase bandpass filters: 1–5 Hz (slope 12 dB/Hz, phase response 180deg/Hz), 5–10 Hz (slope 5 dB/Hz, phase response 52.5 degree/Hz), and 12–18 Hz (slope 1.5 dB/Hz, phase response 23 degree/Hz). The instantaneous analytical amplitude was then obtained from these signals using Hilbert transform. Epochs annotated

visually as oscillatory bouts were selected and signals ordered according to peak amplitude. The signal with the highest amplitude was taken as the index for the given epoch, and the instantaneous amplitude values in all other electrodes were plotted as a function of inter-electrode distance. This yields graphs of amplitude decay as shown in Fig. 2B. Finally, linear regression lines were fitted over the amplitude values within the nearest 5 cm from the index signal (see Fig. 2B) in order to obtain the slopes of amplitude decays, and to compare the decays between frequency bands. (Fig. 2C). The use of several frequency bands is reasoned by the previous studies in adults showing that the spatial extent of an oscillation is proportional to its temporal frequency (Freeman, 2005). In neonatal EEG, the highest frequency range (> 10 Hz) is likely most relevant (Colonnese et al., 2010; Vanhatalo et al., 2005).

#### Simulation experiment

A 4-layer spherical head model was constructed (Fig. 4) to study the effects of source depth and tissue conductivities on the PSDx in scalp EEG. To this end, we defined model dimensions to closely mimic neonatal head (Fig. 4) with a circumference of 36 cm. This leads to the choice of following radii:  $R_1 = 4.9$  cm representing brain;  $R_2 = 5.3$  cm representing CSF;  $R_3 = 5.5$  cm representing skull;  $R_4 = 5.7$  cm representing scalp. Following the recent study of Despotovic et al. (2012), we used the following conductivity values: brain,  $\sigma_1 = 3.3$  mS/cm; CSF,  $\sigma_2 = 17.9$  mS/cm and scalp,  $\sigma_4 = 4.3$  mS/cm. For the skull layer, we tested two conductivities, 2.0 mS/cm and 0.22 mS/cm, to mimic previously published estimates of neonatal and adult conductivities, respectively. To analyze the effect of the dipole depth on PSDx, the simulations were run for dipole depths of 0.85, 1.0 and 1.2 cm from the scalp surface.

In order to mimic our linear array device, we placed 50 electrodes with 2.5 mm spacing on the outer surface of the sphere simulating the scalp EEG points. The sources, point dipoles, were located on radii at different depths from the scalp giving spacing between them slightly less than 3 mm. The linear separation between the dipoles was dependent on the depth of the dipole layer and the 3.0 mm separation between scalp potential points. Each dipole was oriented perpendicular to the tangent of the layer at its point. The dipole intensity was assigned by a

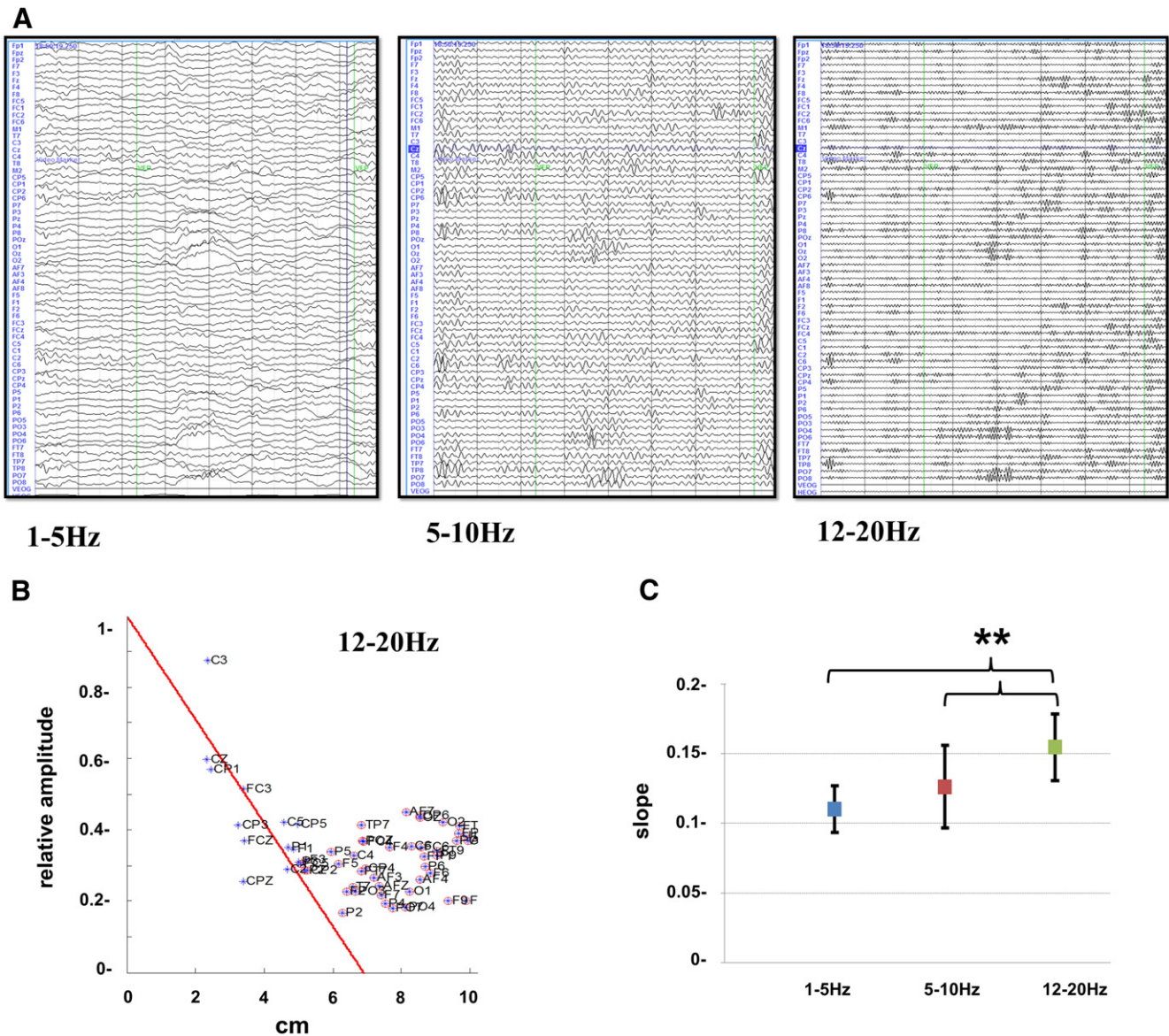


**Fig. 2.** Spatial decay of oscillation amplitudes, the hdEEG experiment. A) Examples of a 64ch EEG tracing after band pass filtering for three different frequency bands. All frequency bands show spatially selective activation bouts, but comparison of the frequency bands shows clearly that the oscillatory bouts become more patchy, i.e. more focal, as the frequency increases. B) Examples of analyses of the spatial decay of oscillation amplitudes at two frequency bands. The instantaneous amplitude of the given frequency band in each electrode is plotted as a function of distance from the electrode in the center of this oscillatory bout (i.e. the signal with the highest amplitude). Note how the amplitudes decay rapidly until they reach the “noise floor” at around 5 cm from the peak. The slope of spatial amplitude decay is calculated from the signals that are within 5 cm from the peak, as shown by the linear fitting in these graphs. C) Summary of the findings of slopes of spatial amplitude decay in different frequency bands. Note the increase in the slope, i.e. steeper decline of amplitudes, at higher frequency bands. Significant differences are shown with asterisks ( $p < 0.01$ ; Mann–Whitney  $U$ -test).

random number generator giving a normal distribution with zero mean and unit standard deviation (SD).

The surface (scalp) potentials of the 4-layer head model were computed using the mathematical expressions described before by Sun (1997) using a Matlab 6.5 software package. The simulated scalp potentials were normalized to zero mean and unit SD by subtracting the mean of the spatial array of data and dividing by the SD. The spatial power spectral densities (PSD<sub>x</sub>) were computed with the 1-D FFT. The procedure was repeated 100 times with independent random intensity patterns of the dipoles, and the PSD<sub>x</sub> values were averaged.

## Results

### Linear array results

Inspection of the raw data from the linear array recordings showed that several EEG events, including single transients or short oscillations,

were strictly confined to a few electrodes only. Fig. 1C shows an example where a rapid oscillation is evident in only about ten electrodes, which implies an extent of only  $10 \times 2.5 = 25$  mm on the scalp. The median PSD<sub>x</sub> calculated over the linear array electrodes shows that the PSD<sub>x</sub> of neonatal EEG follows the canonical form of the background EEG (cf. Freeman et al., 2003) with a flat low-frequency plateau, middle nearly linear  $1/f$  down-slope of log power vs. log frequency, as well as another plateau at a higher frequency range. The finding was qualitatively very similar between the two babies studied. Comparison of signals obtained from different scalp areas shows that the inflection point between the middle and higher frequency range is in all traces at around 0.5–0.8 cycles/cm (Fig. 1E), and the power law ( $1/f$ )-like linear slope in the middle part is similar in all three brain areas. The limited number of spatial points available in such real life recordings does not allow a *tour de force* statistical testing of how strictly the neonatal scalp EEG follows a genuine power law distribution (cf. Clausen et al., 2009), but the similarity between brain areas is notable.

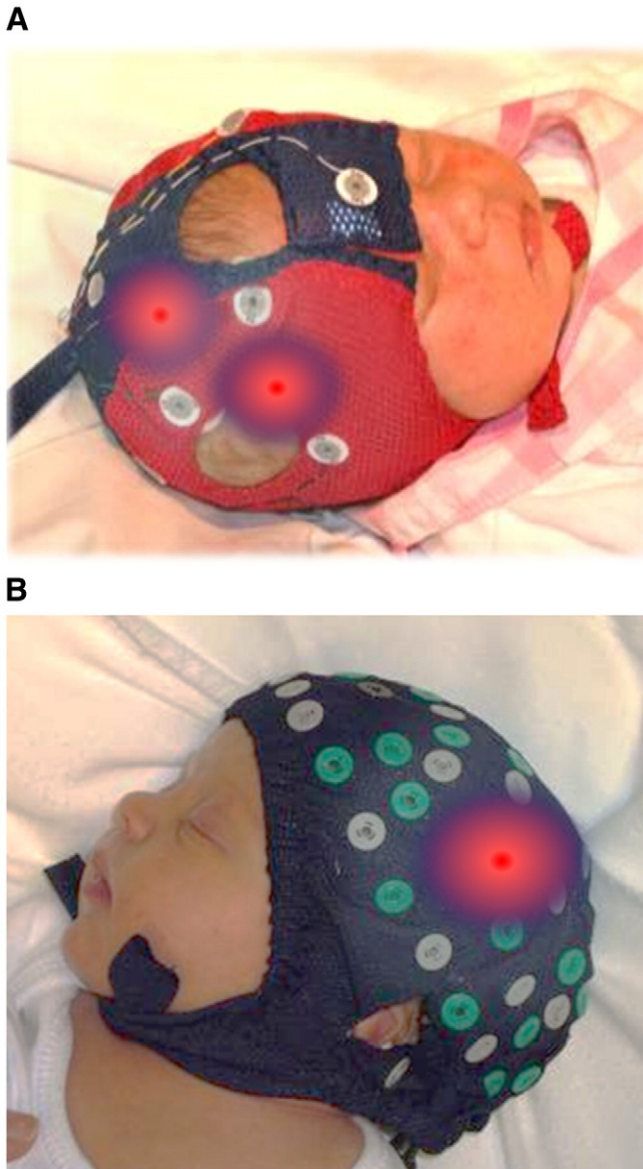


**Fig. 3.** Comparison of conventional and hdEEG recordings. Photographs comparing A) the conventional “full array” neonatal EEG setting (10 electrodes) and B) the hdEEG setting (64 electrodes) used in the present study. The circles with graded colors plotted over the photograph have a diameter of about 4–5 cm. They give a schematic representation of an oscillatory bout that declines to half of its amplitude within the circle, meaning that more than one electrode should be located within this area for its reliable detection. Note how the conventional neonatal EEG severely undersamples the scalp resulting in a high likelihood of missing oscillations of this kind.

There are, however, qualitative differences in the PSDx graphs between the slopes of the higher frequency segments: the signals measured from the parietooccipital area (see Fig. 1A) had steeper slopes than those measured from the parietal or midline areas. The exact anatomical match between the linear array positions and the underlying gyral and sulcal structures or interhemispheric fissures is unavailable. However, our observation suggests that the EEG information content extends to higher spatial frequencies over the cortical areas (parietal and parietooccipital positions) as opposed to the scalp above the interhemispheric fissure (midline) (see Fig. 1E).

#### hdEEG results

Inspection of the raw data (Fig. 2A) shows that i) oscillations at all frequency bands cover only part of the scalp, and ii) oscillations at

higher frequencies tend to appear more “patchy” in the display that shows all electrodes. In other words, the higher frequencies appear to be spatially more limited. To assess the spatial extent of each individual oscillation, we looked at the spatial decay of oscillation amplitudes. The signal with maximal amplitude during the given oscillatory bout was taken as the index signal, and amplitudes of the neighbouring electrodes were plotted as the function of distance. The amplitudes of focal oscillations decline to about half over the nearest 4–6 cm, and then the amplitudes reaches the “noise floor” with no systematic further decline when moving away from the peak (see example in Fig. 2B). Using the linear regression line over the first 5 cm from the index signal to see the slope of the amplitude decay showed that the highest frequencies had the steepest slopes (12–20 Hz:  $0.15 \pm 0.02$  (SEM); 5–10 Hz:  $0.13 \pm 0.03$ ; 1–5 Hz:  $0.11 \pm 0.02$ , see Fig. 2C). The difference between the highest frequency and the lower frequencies was also statistically significant (Mann–Whitney *U*-test:  $p < 0.01$  for 12–20 Hz vs. 5–10 Hz;  $p < 0.01$  for 12–20 Hz vs. 1–5 Hz); however the difference between 1–5 Hz and 5–10 Hz frequency bands was not significant ( $p = 0.17$ ).

#### Simulation results

The averaged PSDx over the 100 PSDx from random dipole intensities is shown in Fig. 4. Using the spherical model with neonatal dimensions (radii and tissue thicknesses) resulted in yielded PSDx graphs with rapid decay between 0.1 and 1.0 c/cm., which is strikingly comparable with the PSDx computed from our linear array recordings (see Fig. 1). Comparison of PSDx generated by using different scalp conductivities and source depths shows a clear effect of both parameters on the PSDx. Increasing the depth of the dipole layer from the most topical position (just below the highest gyri at about 0.85 cm below scalp) towards cortical sites closer to the edges of gyri (up to 1.2 cm below the scalp) substantially decreased the power of PSDx at the spatial frequency range of 0.1 to 1.0 c/cm (note that the power in Fig. 4 is shown in logarithmic scale). This clear trend was seen with both skull layer conductivities. However, increasing skull conductivity near to values recently suggested for neonatal skull (Despotovic et al., 2012) lead to a more than an order of magnitude increase in PSDx at the spatial frequency range of 0.1 to 1.0 c/cm. A closer inspection of the PSDx from our simulation experiment suggests further i) that the slope within 0.1–1.0 c/cm range tends to be steeper with higher conductivity values, and ii) that the higher conductivity is needed to create an apparent lower frequency inflection point at around 0.2 c/cm which is also seen in the real EEG from linear array recordings (Fig. 1E).

#### Discussion

The observations in our study support the notion that the spatial patterning, the amount of unique information in neonatal scalp EEG, is much richer than has been commonly perceived. Notably, the common perception has not been based on knowledge, but has emerged from the way clinical routines were set by the early pioneers of neonatal EEG (reviewed in Andre et al., 2010). It is intriguing in this context, that the idea of rich spatial texture of this kind has been implicitly embedded in the conventional classification of the neonatal EEG. It is well known that neonates may have focal sharp transients or epileptic discharges that only appear in one electrode (see e.g. Andre et al., 2010; Castro Conde et al., 2004; Okumura et al., 2003). If the spatial texture of neonatal EEG was smoothed (i.e., smeared) by volume conduction, such relatively high amplitude transients would be seen in many more electrodes. Our work is hence fully compatible with the implicit knowledge from prior descriptive literature on neonatal EEG, as well as with the prior theoretical analyses on EEG of older infants (Grieve et al., 2003, 2004).

Our observations from the linear array showed that the spatial characteristics of neonatal EEG follow the canonical form of PSDx that is

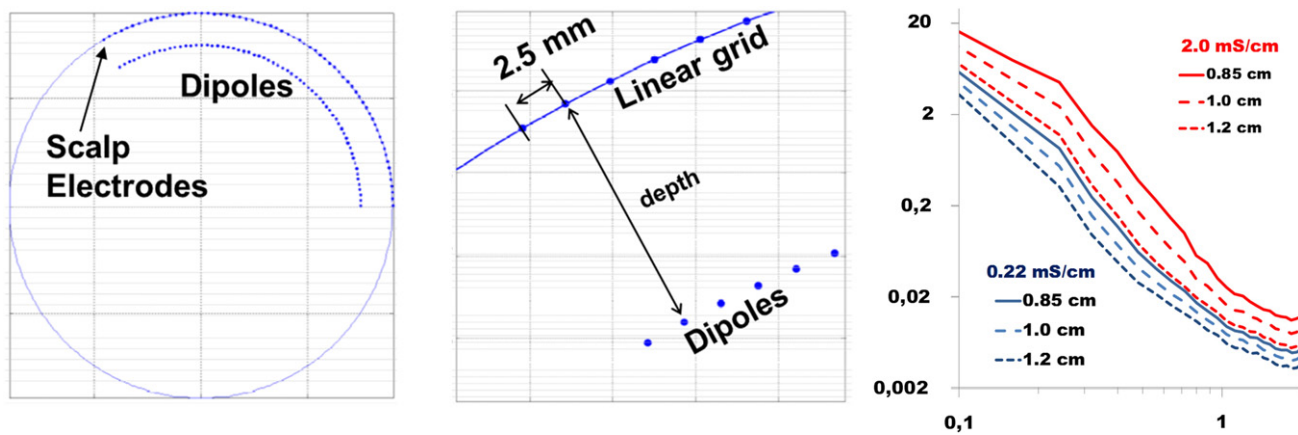


**Fig. 4.** Simulation experiment. Schematic drawing on the left shows the structure of our 4-layer spherical model (left) with neonatal dimensions (circumference ~36 cm). The middle drawing demonstrates the placement of dipole sources on the cortex, as well as the 1-D linear array on the scalp. The graph on the right presents PSDx calculated as an average of 100 simulations in each trace. The upper three PSDx traces (red) represent situation where skull conductivity is set closer to the assumed neonatal value (2.0 mS/cm) with varying depth of the source. The lower three PSDx traces (blue) represent the situation with skull conductivity closer to the assumed adult skull bone conduction (0.22 mS/cm). Note the strong dependency of PSDx, up to orders of magnitude, on both of these parameters.

qualitatively similar to that previously published from comparable adult recordings (Freeman et al., 2003). The essential features of the PSDx for our present study were the inflection points at the lower and higher frequency ends of the middle part of the PSDx with a linear slope (in log-log coordinates). The middle segment delimits the frequency range with the maximal likelihood of finding information content with relevance to brain's electric activity. The inflection point on its right side yields the Nyquist frequency for spatial EEG sampling (see also Freeman et al., 2003). The spatial frequency of this point (~0.5–0.8 c/cm) is equivalent to a wavelength of 1.25–2 cm. Prior work analyzing PSDx from the adult scalp at a comparable temporal frequency range reported the corresponding spatial frequency to be ~0.2–0.4 c/cm, equivalent to a wavelength of 2.5–5 cm (Freeman et al., 2003; Srinivasan et al., 1998). Because the spatial texture of EEG is spatially mostly noncyclic, it would be more robust to have the sample frequency 3–5 times higher than the frequency limit (Barlow, 1993), which would yield interelectrode spacing of about 3–5 mm in neonates and 5–8 mm in adults. Simulations with adult head model have even suggested need for interelectrode spacing as low as 3 mm (see Ramon et al., 2009). The inflection point on the left side (0.5 cycles/cm in Fig. 1, E) indicates the minimum width of an array (2 cm) needed to capture a complete spatial pattern in the EEG in each temporal frequency band (Freeman and Quian Quiroga, 2013).

The hdEEG study showed that each oscillatory bout decayed to the level of the noise floor within about 4 cm (higher frequencies; see Fig. 2B) around its peak location. In order to be detected, multiple electrodes within the given diameter of about 8 cm are required. This would suggest that one needs to have electrodes spaced no more than 2–3 cm apart, or conversely, that each electrode covers roughly about 3 cm of scalp. These spatial considerations are even more important if source localization is an aim. To translate this to actual neonatal EEG recordings, we plotted examples of 3 cm circles on the photographs of newborns with conventional neonatal EEG electrode positions and the hdEEG used in the present study (Fig. 3). The conventional electrode positioning, considered to be “the full neonatal array” (Andre et al., 2010) clearly ignore major parts of brain activity. In particular, electrode coverage of the parietal and centro-temporal areas, the areas with the most developmentally significant rapid oscillations, is so poor that even a majority of focal events may go undetected.

The difference in the estimates of the ideal interelectrode spacing between the linear array and hdEEG study is probably mostly related to the difference in the electrode contact area. The diameter of skin contact area in the hdEEG recordings (i.e. the diameter of the skin gel interface) is around 10–15 mm, whereas it was only 1 mm in our linear

array. The scalp amplitudes within the skin-gel contact area are averaged, so each contact in the hdEEG is spatially averaging four to six consecutive linear array contacts. As a practical example, the local oscillatory bout seen in Fig. 1C (contacts 15–25) spans only 25 mm, and so may be readily ignored by the spatial averaging inherent with the larger electrode contacts. These two ranges of ideal interelectrode estimates should be viewed in the practical context. The theoretical ideal obtained from the linear array recordings sets the upper limit to the density of scalp electrodes as 6–10 mm spacing, but this raises practical challenges in devising appropriate and practical electrode caps. Approaches could include the use of dry electrodes (Toyama et al., 2012), if their mechanical stability can be improved, or a modification of dense EMG arrays (Drost et al., 2006), if they can be developed to establish firm contact with the spherical-shaped baby scalp.

Our observation of the spatially highly varying patterns of neonatal scalp EEG suggests an opportunity for adjustment of the head model used in source localization paradigms. Recent studies have defined head model parameters for neonatal EEG source localization, most importantly tissue conductivities, by estimating the anatomical match between a known brain lesion and the inverse solution of a pathological EEG transient (Despotovic et al., 2012; Roche-Labarbe et al., 2008). This approach assumes that pathological EEG transients are generated within the lesion, which may not always be the case. Our study on the spatial patterning of scalp EEG opens an alternative approach: as shown in our tentative forward model stimulation with spherical model, the head model parameters can be sought by modifying them in a forward solution so that the spatial patterning of the calculated lead field matrix resembles that of empirically observed scalp EEG. Our tentative experiment with spherical model showed clearly how source depth will dramatically affect PSDx power. This observation implies that building a source analysis paradigm by using EEG from deep brain lesions as the anatomical reference (cf. Despotovic et al., 2012; Roche-Labarbe et al., 2008) does likely present a significant bias when aiming to develop and validate source localization paradigms for cortical EEG activity. Moreover, our simulation experiments support the previous suggestions that skull conductivity does strongly affect PSDx. This sets an urgent call for attempts to validate the range of physiologically relevant conductivity estimates to support realistic head models. Intriguingly in this context, electric impedance tomography has been recently developed to a stage that it may offer an alternative paradigm for empirical estimation of *in vivo* tissue conductivities in humans (Esler et al., 2010; Turovets et al., 2008).

The clinical implications of our study must take into account the indication for each EEG study. Some applications such as long term

brain monitoring, will likely not gain from higher spatial resolution. Recent advances in neonatal neuroimaging have clearly highlighted the clinical gain from increased spatial resolution in the anatomical domain. (e.g. Dudink et al., 2012; Fransson et al., 2011; Lodygensky et al., 2010). The next obvious advance will be to define the functional correlate of any altered structure, and this can only be accomplished with improved spatial EEG information.

Finally, the observation of highly varying spatial patterning and power law-like (1/f) linear slope in the spatial spectrum is consistent with the idea that infant cognition may be able to be studied by analysis of the formation of spatiotemporal patterns like cinematic frames (Freeman and Quiroga, 2013) that in some respects resemble “neural avalanches” (Kozma et al., 2013; Plenz and Thiagar, 2007). Capturing these with novel dense array EEG devices, akin to what has been recently achieved with adult EEG (Brockmeier et al., 2012; Panagiotides et al., 2010; Ruiz et al., 2010), may open a novel window to capturing the details of emerging large scale brain processes, such as those related to perception and cognition (Bressler and Menon, 2010).

## Acknowledgments

This work was supported financially by Helsinki University Hospital, Juselius Foundation, and the Foundation of Pediatrics (Lastentautien tutkimussäätiö), the Finnish Academy, and later by the European Community's Seventh Framework Programme European Community FP7-PEOPLE-2009-IOF, grant agreement n°254235. W.F. was supported by a MERIT Award from NIMH.

## References

- Andre, M., Lamblin, M.D., d'Allest, A.M., Curzi-Dascalova, L., Moussalli-Salefranque, F., The, S.N., Vecchierini-Blineau, M.F., Wallois, F., Walls-Esquivel, E., Plouin, P., 2010. Electroencephalography in premature and full-term infants. Developmental features and glossary. *Neurophysiol. Clin.* 40, 59–124.
- Barlow, J.S., 1993. *The Electroencephalogram: Its Patterns and Origins*. MIT Press, Cambridge, MA.
- Beauchemin, M., González-Frankenberger, B., Tremblay, J., Vannasing, P., Martínez-Montes, E., Belin, P., Béland, R., Francoeur, D., Carceller, A.M., Wallois, F., Lassonde, M., 2011. Mother and stranger: an electrophysiological study of voice processing in newborns. *Cereb. Cortex* 21, 1705–1711.
- Bressler, S.L., Menon, V., 2010. Large-scale brain networks in cognition: emerging methods and principles. *Trends Cogn. Sci.* 14, 277–290.
- Brockmeier, A.J., Hazrati, M.K., Freeman, W.J., Principe, J., 2012. Locating global spatial patterns of waveforms during sensory perception in scalp EEG. *Proc IEEE Conf EMBS #2098*, San Diego, 28 Aug–01 Sept.
- Castro Conde, J.R., Martínez, E.D., Campo, C.G., Pérez, A.M., McLean, M.L., 2004. Positive temporal sharp waves in preterm infants with and without brain ultrasound lesions. *Clin. Neurophysiol.* 115, 2479–2488.
- Clauset, A., Shalizi, C.R., Newman, M.E.J., 2009. Power-law distributions in empirical data. *Siam Rev.* 51, 661–703.
- Colonnese, M., Khazipov, R., 2012. Spontaneous activity in developing sensory circuits: implications for resting state fMRI. *Neuroimage* 62, 2212–2221 (Epub ahead of print).
- Colonnese, M.T., Kaminska, A., Minlebaev, M., Milh, M., Bloem, B., Lescure, S., Moriette, G., Chiron, C., Ben-Ari, Y., Khazipov, R., 2010. A conserved switch in sensory processing prepares developing neocortex for vision. *Neuron* 67, 480–498.
- Despotovic, I., Cherian, P.J., De Vos, M., Hallez, H., Deburchgraeve, W., Govaert, P., Lequin, M., Visser, G.H., Swarte, R.M., Vansteenkiste, E., Van Huffel, S., Philips, W., 2012. Relationship of EEG sources of neonatal seizures to acute perinatal brain lesions seen on MRI: a pilot study. *Hum. Brain Mapp.* <http://dx.doi.org/10.1002/hbm.22076> (Epub ahead of print).
- Drost, G., Stegeman, D.F., van Engelen, B.G., Zwarts, M.J., 2006. Clinical applications of high-density surface EMG: a systematic review. *J. Electromyogr. Kinesiol.* 16, 586–602.
- Dudink, J., Counsell, S.J., Lequin, M.H., Govaert, P.P., 2012. DTI reveals network injury in perinatal stroke. *Arch. Dis. Child. Fetal Neonatal Ed.* 97, F362–F364.
- Esler, B., Lyons, T., Turovets, S., Tucker, D., 2010. Instrumentation for low frequency EIT studies of the human head and its validation in the phantom experiments. *J. Phys. Conf. Ser.* 224, 012007.
- Fifer, W.P., Grieve, P.G., Grose-Fifer, J., Isler, J.R., Byrd, D., 2006. High-density electroencephalogram monitoring in the neonate. *Clin. Perinatol.* 33, 679–691.
- Fransson, P., Aden, U., Blennow, M., Lagercrantz, H., 2011. The functional architecture of the infant brain as revealed by resting-state fMRI. *Cereb. Cortex* 21, 145–154.
- Freeman, W.J., 2005. Origin, structure, and role of background EEG activity. Part 3. Neural frame classification. *Clin. Neurophysiol.* 116, 1118–1129.
- Freeman, W.J., Quiroga, R., 2013. *Imaging Brain Function with EEG: Advanced Temporal and Spatial Imaging of Electroencephalographic Signals*. Springer, New York. <http://dx.doi.org/10.1007/978-1-4614-4984-3>.
- Freeman, W.J., Rogers, L.J., Holmes, M.D., Silbergeld, D.L., 2000. Spatial spectral analysis of human electrocorticograms including the alpha and gamma bands. *J. Neurosci. Methods* 95, 111–121.
- Freeman, W.J., Holmes, M.D., Burke, B.C., Vanhatalo, S., 2003. Spatial spectra of scalp EEG and EMG from awake humans. *Clin. Neurophysiol.* 114, 1053–1068.
- Grieve, P.G., Emerson, R.G., Fifer, W.P., Isler, J.R., Stark, R.I., 2003. Spatial correlation of the infant and adult electroencephalogram. *Clin. Neurophysiol.* 114, 1594–1608.
- Grieve, P.G., Emerson, R.G., Isler, J.R., Stark, R.I., 2004. Quantitative analysis of spatial sampling error in the infant and adult electroencephalogram. *Neuroimage* 21, 1260–1274.
- Hanganu-Opatz, I.L., 2010. Between molecules and experience: role of early patterns of coordinated activity for the development of cortical maps and sensory abilities. *Brain Res. Rev.* 64, 160–176.
- Khazipov, R., Luhmann, H.J., 2006. Early patterns of electrical activity in the developing cerebral cortex of humans and rodents. *Trends Neurosci.* 29, 414–418.
- Kozma, R., Puljic, M., Freeman, W.J., 2013. Thermodynamic model of criticality in the cortex based on EEG/ECOG data. Chapter In: Plenz, D., Niebur, E. (Eds.), *Criticality in Neural Systems*. John Wiley & Sons, Bethesda. <http://escholarship.org/uc/item/43q8x3zb>.
- Lodygensky, G.A., Vasung, L., Sizonenko, S.V., Hüppi, P.S., 2010. Neuroimaging of cortical development and brain connectivity in human newborns and animal models. *J. Anat.* 217, 418–428.
- Okumura, A., Hayakawa, F., Kato, T., Maruyama, K., Kubota, T., Suzuki, M., Kidokoro, H., Kuno, K., Watanabe, K., 2003. Abnormal sharp transients on electroencephalograms in preterm infants with periventricular leukomalacia. *J. Pediatr.* 143, 26–30.
- Panagiotides, H., Freeman, W.J., Holmes, M.D., Pantazis, D., 2010. Behavioral states may be associated with distinct spatial patterns in electrocorticogram (ECOG). *Cogn. Neurodyn.* 5, 55–66.
- Plenz, D., Thiagar, T.C., 2007. The organizing principles of neural avalanches: cell assemblies in the cortex. *Trends Neurosci.* 30, 101–110.
- Ramon, C., Freeman, W.J., Holmes, M., Ishimaru, A., Haeisen, J., Schimpf, P.H., Rezvani, E., 2009. Similarities between simulated spatial spectra of scalp EEG, MEG and structural MRI. *Brain Topogr.* 22, 191–196.
- Roche-Labarbe, N., Aarabi, A., Kongolo, G., Gondry-Jouet, C., Dümpelmann, M., Grebe, R., Wallois, F., 2008. High-resolution electroencephalography and source localization in neonates. *Hum. Brain Mapp.* 29, 167–176.
- Ruiz, Y., Pockett, S., Freeman, W.J., Gonzales, E., Li, G., 2010. A method to study global spatial patterns related to sensory perception in scalp EEG. *J. Neurosci. Methods* 191, 110–118.
- Scherg, M., Ille, N., Bornfleth, H., Berg, P., 2002. Advanced tools for digital EEG review: virtual source montages, whole-head mapping, correlation, and phase analysis. *J. Clin. Neurophysiol.* 19, 91–112.
- Srinivasan, R., Tucker, D.M., Murias, M., 1998. Estimating the spatial Nyquist of the human EEG. *Behav. Res. Methods Instrum. Comput.* 30, 8–19.
- Stjerna, S., Voipio, J., Metsäranta, M., Kaila, K., Vanhatalo, S., 2012. Preterm EEG: A Multimodal Neurophysiological Protocol. *J. Vis. Exp.* e3774. <http://dx.doi.org/10.3791/3774>.
- Sun, M., 1997. An efficient algorithm for computation of multishell spherical volume conductor models in EEG dipole source localization. *IEEE Trans. Biomed. Eng.* 44, 1243–1252.
- Tokariyev, A., Palmu, K., Lano, A., Metsäranta, M., Vanhatalo, S., 2012. Phase synchrony in the early preterm EEG: development of methods for estimating synchrony in both oscillations and events. *Neuroimage* 60, 1562–1573.
- Toyama, S., Takano, K., Kansaku, K., 2012. A non-adhesive solid-gel electrode for a non-invasive brain-machine interface. *Front. Neurol.* 3, 114 (Epub 2012 Jul 18).
- Tucker, D.M., Brown, M., Luu, P., Holmes, M.D., 2007. Discharges in ventromedial frontal cortex during absence spells. *Epilepsy Behav.* 11, 546–557.
- Turovets, S.I., Poolman, P., Salman, A., Malony, A., Tucker, D., 2008. Noninvasive conductivity extraction for high-resolution EEG source localization. *Int Conference in Biomedical Engineering and Informatics, IEEE*, pp. 386–393.
- Vanhatalo, S., Kaila, K., 2006. Development of neonatal EEG activity: from phenomenology to physiology. *Semin. Fetal Neonatal Med.* 11, 471–478.
- Vanhatalo, S., Kaila, K., 2010. Spontaneous and evoked activity in the early human brain. In: Lagercrantz, H., Hanson, M.A., Ment, L.R., Peebles, D.M. (Eds.), *The Newborn Brain: Neuroscience & Clinical Applications*, 2nd edition. Cambridge University Press, pp. 229–243 (Chapter 15).
- Vanhatalo, S., Palva, J.M., Andersson, S., Rivera, C., Voipio, J., Kaila, K., 2005. Slow endogenous activity transients and developmental expression of K<sup>+</sup>–Cl<sup>–</sup> cotransporter 2 in the immature human cortex. *Eur. J. Neurosci.* 22, 2799–2804.
- Vanhatalo, S., Metsäranta, M., Andersson, S., 2008. High-fidelity recording of brain activity in the extremely preterm babies: feasibility study in the incubator. *Clin. Neurophysiol.* 119, 439–445.